Journal of the Korean Physical Society, Vol. 59, No. 5, November 2011, pp. 3069∼3073

Determination of the Temperature Dependence of the Magnetic Anisotropy Constant in Magnetite Nanoparticles

Sunghyun YOON*
Department of Physics, Gunsan National University, Gunsan 573-701, Korea

(Received 10 October 2011)

The temperature dependence of the effective magnetic anisotropy constant, $K(T)$, of Fe_3O_4 (magnetite) nanoparticles is obtained based on SQUID (superconducting quantum interference device) magnetometry. The variation of the blocking temperature, T_B, as a function of particle radius, r, is first determined by associating the particle size distribution and the anisotropy energy barrier distribution deduced from the hysteresis curve and from the magnetization decay curve, respectively. Finally, the magnetic anisotropy constant at each temperature is calculated from the relation between r and T_B. The resultant effective magnetic anisotropy constant $K(T)$ decreases markedly with increasing temperature from 5.9×10^5 J/m^3 at 5 K to 1.1×10^4 J/m^3 at 280 K.

PACS numbers: 75.30.Gw, 75.75.+a
Keywords: Magnetic nanoparticles, Magnetic anisotropy constant
DOI: 10.3938/jkps.59.3069

I. INTRODUCTION

The dynamics of the relaxation behavior of superparamagnetic nanoparticles is mainly governed by the anisotropy constant, as well as the composition, size and surfactant of the particles [1]. The magnetization vector in a single-domain particle tends to align along a direction, called the easy axis, that yields the minimum magnetocrystalline anisotropy energy. This anisotropy energy acts as an energy barrier that limits free rotation of the magnetic moments away from the easy axis. When the energy barrier is overcome thermally, the magnetization can reverse its direction rapidly, exhibiting a superparamagnetic relaxation. For non-interacting particles with uniaxial anisotropy, the relaxation time for the reversal process is described by the Néel-Arrhenius equation [2]

$$\tau = \tau_0 \exp\left(\Delta E_A / k_B T\right), \quad (1)$$

where k_B is Boltzmann's constant, T is the absolute temperature, and τ_0 is an attempt time on the order of 10^{-9} – 10^{-13} s. $\Delta E_A = KV$ is the anisotropy energy barrier, where K is the effective anisotropy constant and V is the particle volume. The temperature at which this relaxation time τ equals the measurement time τ_m and at which the particle system goes into the superparamagnetic region is the blocking temperature T_B.

Since the magnetic anisotropy constant determines the energy barrier for the coherent rotation of the particle moment, its characterization is very important for practical applications of the relaxation mechanism in superparamagnetic nanoparticles. Several experimental techniques are currently employed to infer the magnitude of the magnetic anisotropy constant K. The most typical way is to obtain T_B from field cooled (FC) - zero field cooled (ZFC) magnetization measurements and to determine the K value by using the equation $K = 25 k_B T_B / \langle V \rangle$ [3,4]. Here, $\langle V \rangle$ is the median volume of the particles, and the factor 25 is a typical $\ln(\tau_m/\tau_0)$ value for conventional magnetometry. It is a quick and convenient method widely used recently for highly-monodispersed nanoparticles [5]. Another method frequently used is to obtain the relaxation times from two different tools with different measuring time scales and to solve for K and τ_0 by using Eq. (1) [6,7]. Besides, the K value can be deduced either from the coercivity and the saturation magnetization in the hysteresis loop measurement [8] or from the low-temperature variation of the hyperfine magnetic field by using Mössbauer spectroscopy [9]. One can alternatively use the ac method, in which the temperature dependence of the ac susceptibility is measured within a range of the frequency f [10]. In this case, $\ln(1/f)$ shows a linear relationship to the reciprocal of the temperature at which the susceptibility is a maximum, from whose slope one can determine the anisotropy constant. However, most of the works mentioned above use only the average particle size in their calculations, not taking the particle size distribution into account as a whole. Thus, they get the magnetic anisotropy as a constant independent of temperature, although a change in the magnetic anisotropy

*E-mail: shyoon@kunsan.ac.kr; Fax.: +82-63-469-4561

with temperature is a well-known physical phenomenon in magnetic materials [11,12]. An analysis under the assumption that the magnetic anisotropy is constant in a temperature range where it is indeed changing is already known to produce erroneous results [13].

There are relatively few experimental studies that determine the magnetic anisotropy throughout a wide temperature range, despite its significance for understanding the relaxation behavior of superparamagnetic nanoparticles. In this study, a very simple but intuitive and conceptual method for determining the temperature dependence of the anisotropy constant $K(T)$ in superparamagnetic nanoparticles is introduced. Finally, the validity of the method is tested by applying it to magnetite nanoparticles, and the impact of inter-particle interaction on the anisotropy is discussed based on the characteristics of the method.

II. EXPERIMENT

Magnetite nanoparticles were synthesized by using conventional co-precipitation of $FeCl_2$ and $FeCl_3$ in a strong alkaline medium [14,15]. Stoichiometric ratios of $FeCl_3{\cdot}6H_2O$ and $FeCl_2{\cdot}4H_2O$ were combined to form an aqueous solution and were slowly added to excess a 1-M aqueous NH_3 solution with vigorous stirring at 80 °C. The black precipitate thus formed was gathered by using magnetic decantation. After the precipitate had been washed several times, 25% tetramethylammonium hydroxide was added for surface coating. The final product was collected and redispersed in water to get a black colloidal solution of magnetite. In order to prevent probable oxidation, all the processes were carried out under a flow of N_2 gas.

The particle size and morphology were examined by using the transmission electron microscopy (TEM). The DC magnetization curve, including the initial curve for 100 μL of the ferrofluid sample, was measured by using a superconducting quantum interference device (SQUID) magnetometer. In order to get the blocking temperature distribution, we measured the temperature dependence of the magnetization decay M_{TD} of the sample as well. For this measurement, the sample was cooled from room temperature to 5 K in a magnetic field of 100 G. Then, the applied field was turned off, and the remanent magnetization was measured for stepwise increases in the temperature.

III. RESULTS AND DISCUSSION

A typical TEM image of the particles is presented in Fig. 1, in which the particles have an irregular morphology with some size distribution. The nominal diameter of the sample, as obtained from an image analysis of the TEM micrograph, was 10 nm.

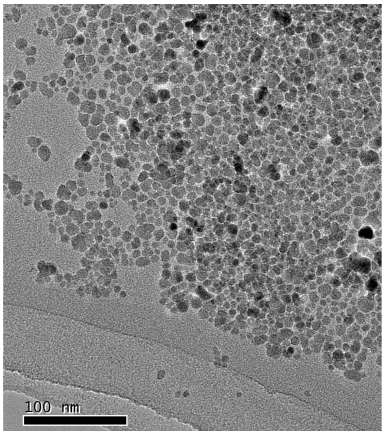

Fig. 1. TEM image of the magnetite nanoparticles.

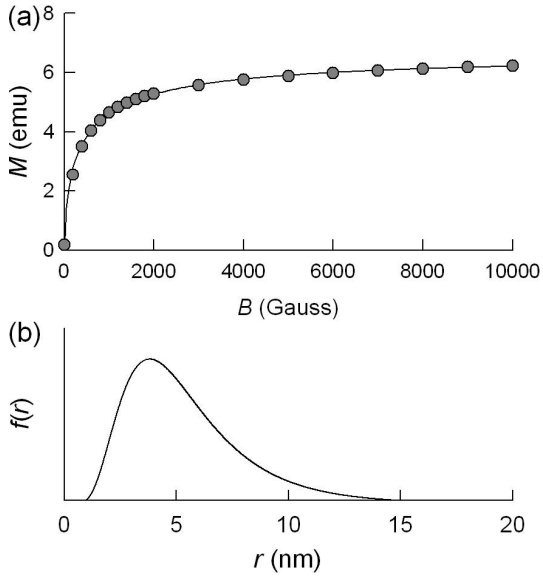

Fig. 2. (a) Results of M *vs.* H curve analysis for Eq. (2) and (b) the corresponding log-normal particle size distribution $f(r)$ for the magnetite nanoparticles.

The room-temperature hysteresis curve for the sample shows a superparamagnetic behavior with no hysteresis. In order to estimate the particle size and its distribution, we fitted the first quadrant part of these hysteresis curves (Fig. 2(a)) to the classical Langevin function $L(H,r)$ weight-averaged with the log-normal particle size distribution $f(r)$ as in the following equation [16,17]:

$$M(H) = \varepsilon M_S \int L(H,r) f(r) dr, \tag{2}$$

where M_S is the saturated magnetization of the single domain particles and ϵ is the volume fraction of the sample. The optimum median radius was found to be 5.4 nm; the resultant distribution $f(r)$ is shown in Fig. 2(b).

The anisotropy energy barrier distribution $f_A(T)$ was obtained from the temperature dependence of the magnetization decay M_{TD} of the sample as depicted in Fig. 3,

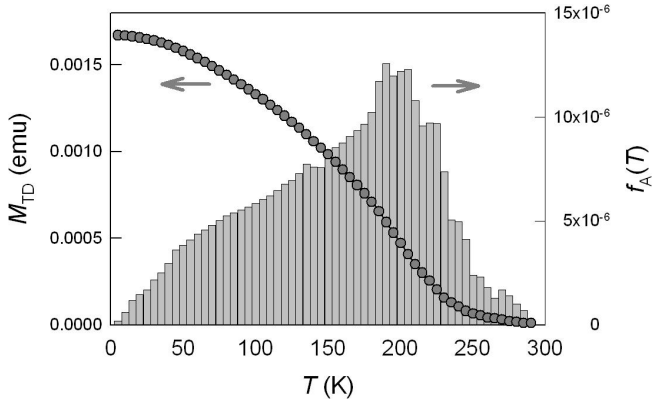

Fig. 3. Temperature dependence of the magnetization decay for magnetite nanoparticles cooled under a magnetic field of 100 G. The histogram is the anisotropy energy barrier distribution $f_A(T)$ deduced from Eq. (3).

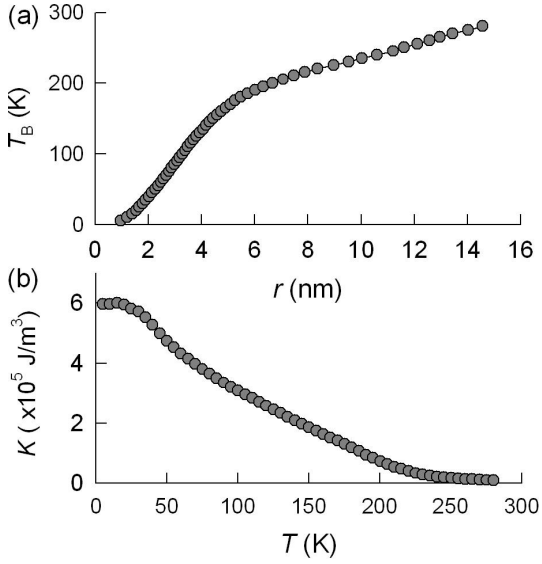

Fig. 4. (a) T_B as a function of r obtained programmatically from the analysis of Eq. (4) and (b) the temperature dependence of the effective anisotropy constant $K(T)$ for magnetite nanoparticles calculated from Eq. (5).

in which the magnetization decreases with increasing temperature and finally vanishes at 280 K. In view of the fact that the unblocked particles cannot contribute to the residual magnetization, more and more particles are getting unblocked with increasing temperature, and 280 K is the temperature at which the unblocking of the largest particles in the sample takes place. Consequently, M_{TD} at a given temperature is a measure of the fraction of nanoparticles in the sample that are still blocked within the measurement time scale τ_m. Since this fraction decreases gradually as the energy barrier is overcome thermally with increasing temperature, the slope of the magnetization decay curve at any temperature gives the energy barrier distribution $f_A(T)$ [17]:

$$f_A(T) \propto -\left.\frac{dM_{TD}}{dT}\right|_T . \tag{3}$$

The histogram in Fig. 3 shows the resultant energy barrier distribution $f_A(T)$. If the anisotropy constant were temperature independent, the anisotropy energy barrier distribution $f_A(T)$ would have had the same log-normal form as the size distribution $f(r)$. Actually, some studies report that this is indeed the case [18], but this does not always hold, in general [19]. From Fig. 2(b) and the histogram in Fig. 3, $f_A(T)$ can be seen to skew to the right whereas $f(r)$ skews to the left (ordinary log-normal distribution). This discrepancy can be explained if a temperature dependence is introduced into the anisotropy constant.

Now, we have two different distributions at hand, so the next step is to associate them to extract information on the temperature dependence of the anisotropy constant. Immediately after the cooling down to 5 K under an external magnetic field is achieved, most of the particle moments are blocked along the field direction. As the temperature increases higher and higher, larger and larger particles in the distribution $f(r)$ are unblocked and begin flipping faster than the measuring time scale τ_m. This means more and more of the energy barrier in the distribution $f_A(T)$ is overcome. To be more specific, assume x% of the sample is in the superparamagnetic state for a given particle size distribution. Then, one can obtain an estimate of the corresponding blocking temperature from the distribution of the energy barrier by evaluating the critical temperature at which the same x% of the cumulative energy barrier is overcome. Mathematically, this can be represented as

$$\int_0^{r(T_B)} f(r')dr' = \int_5^{T_B} f_A(T')dT', \tag{4}$$

where $r(T_B)$ is the radius of the particles whose blocking temperature is T_B.

By taking two equal quantiles from each of the distributions, one can get a relation between the particle radius r and the corresponding blocking temperature T_B, as shown in Fig. 4(a). If the anisotropy constant K is a constant in temperature, T_B should show a simple steep increase with increasing r. However, T_B shows a trend toward saturation, which strongly suggests the possibility that K should decrease with increasing temperature. Fernandez reported a similar saturation behavior in $T_B(r)$ by introducing temperature-dependent magnetic anisotropy constants for Ni and Co nanoparticles [13]. Substituting the values of r and T_B into Eq. (1) and rearranging it, we can estimate the anisotropy constant at a given temperature as

$$K(T) = \frac{k_B T}{V(r)} \ln\left(\frac{\tau_m}{\tau_0}\right), \tag{5}$$

where τ_m was set to 100 s, which is suitable for conventional magnetometry. In order to go further, however,

one needs to decide the other unknown parameter τ_0 in Eq. (5) . During the programmatic process of the calculation, the value of τ_0 was chosen in such a way that the anisotropy constant at 280 K becomes 1.1×10^4 J/m^3, as reported in the literature [20]. This was obtained for $\tau_0 = 1.3 \times 10^{-12}$ s, which is somehow shorter than, but is still within, the values reported in the literature [6,22]. If this study is backed up by a complementary measurement with a different characteristic time scale, such as Mössbauer spectroscopy, one can get a precise value of τ_0, as well.

The resultant temperature dependence of the anisotropy constant for the present sample is represented in Fig. 4(b). Note that neither a median volume deduced from $f(r)$ or a TEM micrograph, nor a median blocking temperature deduced from $f_A(T)$ was used in the course of the calculation. The anisotropy constant obviously decreases with increasing temperature. The anisotropy constant has often been empirically assumed to decrease linearly with temperature as $K(T) = K(0)(1 - T/T_A)$, where $K(0)$ and T_A are the anisotropy at 0 K and the temperature corresponding to zero anisotropy, respectively [23,24]. The anisotropy constant in Fig. 4(b) exhibits, however, a more complicated variation with temperature. At this stage, the physical origin for the nontrivial variation is not clear. In view of the reduced slope of the blocking temperature variation in Fig. 4(a), a reversal of the magnetization in larger particles ($r > 6$ nm) may take place through an incoherent rotation inside the particles. However, this needs to be verified further.

The anisotropy constant at 5 K is more than one order of magnitude larger than that at 280 K in the present study. Such an enhancement in the anisotropy constant at low temperatures has also been reported in previous studies [24]. The enhanced anisotropy at low temperature in the present study may well be attributed to an extra energy barrier resulting from an inter-particle interaction between smaller particles that get unblocked at low temperature [25]. The underlying physics of the method introduced in this study is based on the blocking/unblocking mechanism of single domain particles according to their sizes, which allows this method to more sensitively reflect the size distribution. Smaller particles are easily unblocked at lower temperatures. Moreover, because smaller particles have a larger surface/volume ratio, they are especially susceptible to inter-particle effects through the interaction of surface magnetic moments with those of neighboring grains. Putting these together, one can conclude that a contribution from inter-particle interactions in smaller particles may result in the enhanced K at low temperatures in Fig. 4(b). In addition, it is also noteworthy that a high-quality monodispersed sample was not required for this study. Rather, a polydispersed sample with a moderate size distribution width was preferred so as to obtain a variation of the anisotropy constant over a wider temperature range.

IV. CONCLUSION

The temperature dependence of the anisotropy constant for Fe_3O_4 nanoparticles was studied through an analysis of the freezing dynamics of particles of different sizes. The temperature dependence of the magnetic anisotropy constant, $K(T)$, for nanoparticles was determined from the particle size distribution and the anisotropy energy barrier distribution deduced from magnetometry measurements. Under the simple assumption that the superparamagnetic fraction of the cumulative area in the particle size distribution at a temperature is equal to the fraction of anisotropy energy barrier overcome at that temperature in the anisotropy energy barrier distribution, we were able to get a relation between r and T_B, from which the temperature dependence of the magnetic anisotropy constant was determined. The resultant magnetic anisotropy constant decreased monotonically with increasing temperature. The anisotropy constant at low temperatures was far more than one order of magnitude larger than that at 280 K, indicating the effects of inter-particle interactions in the surface, which is known to be more pronounced for smaller particles. This was anticipated because the measurements were done with a dried powder. In this respect, a supplementary experiment with a sample free of inter-particle interactions is required for comparison.

ACKNOWLEDGMENTS

This work was supported by Basic Science Research Program (2010-0023413) through the National Research Foundation (NRF) of Korea.

REFERENCES

[1] K. M. Krishnan, IEEE Trans. Magn. **46**, 2523 (2010).
[2] L. Néel, Ann. Geophys. **5**, 99 (1949).
[3] P. Guardia, B. Batlle-Brugal, A. G. Roca, O. Iglesias, M. P. Morales, C. J. Serna, A. Labarta and X. Batlle, J. Magn. Magn. Mater. **316**, e756 (2007).
[4] R. Venugopal, B. Sundaravel, W. Y. Cheung, I. H. Wilson, F. W. Wang and X. X. Zhang, Phys. Rev. B **65**, 014418 (2001).
[5] T. Hyeon, Y. Chung, J. Park, S. S. Lee, Y-W. Kim and B. H. Park, J. Phys. Chem. B **106**, 6831 (2002).
[6] D. P. E. Dickson, N. M. K. Reid, C. Hunt, H. D. Williams, M. El-Hilo and K. O'Grady, J. Magn. Magn. Mater. **125**, 345 (1993).
[7] A. J. Rondinon, A. C. S. Samia and Z. J. Zhang, Appl. Phys. Lett. **76**, 3624 (2000).
[8] T. Ibusuki, S. Kojima, O. Kitakami and Y. Shimada, IEEE Trans. Magn. **37**, 2223 (2001).
[9] S. Mørup, J. Magn. Magn. Mater. **37**, 39 (1983).

[10] V. B. Barberta, R. F. Jardim, P. K. Kiyohara, F. B. Effenberg and L. M. Rossi, J. Appl. Phys. **107**, 073913 (2010).
[11] J. Kanamori, *Magnetism*, edited by G. T. Rado and H. Suhl (Academic Press, NY, 1963), Vol. 1, Chap. 4.
[12] H. Shenker, Phys. Rev. **107**, 1246 (1957).
[13] D. de J. Fernandez, Phys. Rev. B **72**, 054438 (2005).
[14] Y. S. Kang, S. Risbud, J. F. Rabolt and P. Stroeve, Chem. Mater. **8**, 2209 (1996).
[15] G. F. Goya, T. S. Berquo, F. C. Fonseca and M. P. Morales, J. Appl. Phys. **94**, 3520 (2003).
[16] R. W. Chantrell, J. Popplewell and S. W. Charles, IEEE Trans. Magn. **14**, 975 (1978); K. Yakushiji, S. Mitani, K. Takanashi, J-G. Ha and H. Fujimori, J. Magn. Magn. Mater. **212**, 75 (2000).
[17] A. J. Rondinon, A. C. S. Samia and Z. J. Zhang, J. Phys. Chem. B **103**, 6876 (1999).
[18] D. Peddis, C. Cannas, A. Musinu and G. Piccaluga, Chem. Eur. J. **15**, 7822 (2009).
[19] J. C. Denardin, A. L. Brandl, M. Knobel, P. Panissod, A. B. Pakhomov, H. Liu and X. X. Zhang, Phys. Rev. B **65**, 064422 (2002).
[20] G. Bate, *Ferromagnetic Materials* (North-Holland, Amsterdam,1980), Vol. 2, p. 431.
[21] S. Mørup, F. Bødker, P. V. Hendriksen and S. Linderoth, Phys. Rev. B **52**, 287 (1995).
[22] N. Hanh, O. K. Quy, N. P. Thuy, L. D. Tung and L. Spinu, Physica B **327**, 382 (2003).
[23] J. F. Hochepied and M. P. Pileni, J. Appl. Phys. **87**, 2472 (2000).
[24] S-H. Yoon and K. M. Krishnan, J. Appl. Phys. **109**, 07B534 (2011).
[25] F. Bødker, S. Mørup and S. Linderoth, Phys. Rev. Lett. **72**, 282 (1994).